Testing the Conjugative Properties of Benzodithiophene and Benzotrithiophene in Charge Transfer Multi(Ferrocenyl) Systems

Serena Rossi, Annalisa Bisello, Roberta Cardena, and Saverio Santi*

Dipartimento di Scienze Chimiche, Università degli Studi di Padova, via Marzolo 1, 35131 Padova, Italy.

Supporting Information Placeholder

ABSTRACT: The charge transfer properties of the mono-, di-, and tricationic derivatives of bis(ferrocenyl)benzodithiophene and tris(ferrocenyl)benzotrithiophene were investigated. The cations were generated by chemical oxidation using ferrocenium(BF_4) and acetylferrocenium(BF_4) as the oxidative agents, and monitored in the visible and NIR regions. By changing the supporting electrolyte from [nBu$_4$N][PF_6] to [nBu$_4$][B(C_6F_5)$_4$] we were able to selectively generate the monocationic species of bis and triferrocenyl complexes. The redox and optical properties of the cationic derivatives were rationalized by an in-depth electrochemical and optical study. The comparison with the results previously obtained for the structurally related bis(ferrocenyl)-*s*-indacene and tris(ferrocenyl)-trindene allowed for the evaluation of the huge influence of thiolation on the metal-metal electronic coupling.

INTRODUCTION

Thiophene-based π-conjugated oligomers and polymers have been widely investigated as organic semiconductors.[1-3] Owing to their appropriate characteristics (electronic, optical, and magnetic properties) for producing electronic and optical devices, (multi)thiophene fused-aromatic compounds are attracting growing interest as promising electronic materials for organic conductors,[4] organic light-emitting diode,[5] photovoltaic cells[6] and field-effect transistors.[7]

Moreover, the extended and planar π-conjugation associated with the electron-rich structure of the fused heterocycles enables them to exhibit strong stacking through intermolecular interactions which confer enhanced hole-carrier mobilities.[8] In addition, thiophene-based oligomers and polymers have been shown to be naturally stable and robust.

In the last decade, considerable interest has been devoted towards benzo[1,2-*b*:4,5-*b*']dithiophene (**BDT**) and benzo[1,2-*b*:3,4-*b*':5,6-*b*'']trithiophene (**BTT**) as potential π-cores for organic semiconductors (Chart 1).

Chart 1. Fused-thiophene compounds.

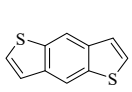

BDT

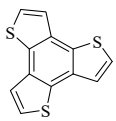

BTT

BDT is a linear-shaped fused dithiophene with two identical thiophene moieties with C_{2h} symmetry which has been widely used in semiconductors.[9] It was first employed in photovoltaic polymers by Hou and coworkers in 2008,[10] and became one of the most successful building blocks in highly efficient organic solar cells[11] and field effect transistors,[3a] which have been proven to match the desirable requirements for these devices.[12]

BTT is a sulfur-rich and extended π-system possessing a planar structure with three identical thiophene rings fused to a central benzene ring,[3,13] which has been studied thoroughly and used as a core for the construction of star-shaped oligomers and dendrimers.[14] Its C_{3h} symmetry takes advantage of the intermolecular π–π and S···S interactions responsible of the efficient hole-transporting properties of its materials.[15a]

BTT is one of the most promising candidates for high performance photovoltaic devices,[6d,15-17] field effect transistors,[7a-c, 14c] electrochromics[14d] and charge carrier discotic liquid crystals.[18] Interestingly, in very recent works Martín, Nazeeruddin and co-workers reported new star-shaped families of hole-transporting (HTMs) materials based on **BTT** isomers as central cores bearing *p*-methoxydi- and triphenylamines, which exhibited remarkable power conversion efficiencies (PCEs) when used in organometal trihalide perovskites solar cells.[14]

The set-up of multicomponent compounds with specific redox, optoelectronic and conductive properties is presently essential for modern technology.[19] Ferrocene is one of the most employed organometallic components. Its stability, redox properties, specific electron donor character and well-developed functionalization chemistry make it a primary candidate for testing the electronic properties in conjugated systems. Especially, (multi)ferrocenyl systems with conjugated spacer groups exhibit multielectron redox chemistry and are of particular interest owing to their unpaired electron migration properties.[20]

Examples of bimetallic **BDT** are rather rare.[21] The bis(ferrocenyl) derivative, 2,6-bis(ferrocenyl)benzo[1,2-*b*:4,5-*b''*]dithiophene (**1**), was previously synthesized by Negishi ferrocenylation of the appropriate bromo-substituted **BDT**.[21d] Very recently, we described a more efficient approach to prepare **1** in good yield and short reaction time via one-pot CuI/TMEDA catalyzed two fold thioannulation with sodium sulfide of 1,4-dibromo-2,5-bis(ethynylferrocenyl)benzene,[22]

obtained by Sonagashira-coupling of 1,4-dibromo-2,5-diiodobenzene.[23]

Similarly, we prepared the tris(ferrocenyl) derivative of **BTT**, the 2,5,8-tris(ferrocenyl)benzo[1,2-*b*:3,4-*b'*:5,6-*b''*]trithiophene (**2**), the first examples of organometallic complex of **BTT** reported so far (Chart 2).

Chart 2. BDT and BTT ferrocenyl complexes

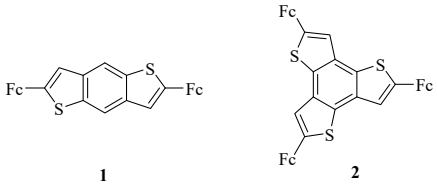

1 **2**

Multi(ferrocenyl) compounds were intensely studied because conjugated organic chains containing Fe^{II}/Fe^{III} couples of the ferrocenyl group can be used as switchable arrays in molecular electronics, quantum cellular automata, optoelectronic materials, and biochemistry for application in redox or photonic devices.[24]

The mixed-valence states having at least two equivalent ferrocenyl groups in different oxidation states are excellent standards for the study of intramolecular charge transfer. Actually, the formation of mixed-valence species is often accountable for the aforementioned performances. The factors affecting the formation, stability, and nature of mixed-valence states in multi(ferrocenyl) derivatives were methodically examined.[20,21,25] In particular, it was found that the electron transfer mechanism in mixed-valence intermediates is mostly based on the Marcus–Hush theory.[26]

In this work, we present the results of an in-depth experimental and theoretical study on the optical and redox properties of the cationic derivatives of compounds **1** and **2** (Chart 2). The comparison with the results previously obtained for the structurally related 1,5-dihydro- and 1,7- and-2,6-diferrocenyl-*s*-indacenes[20h] (**3**) and 4,7- and 6,7-dihydro-2,5,8-triferrocenyl-trindenes[20d] (**4**) complexes (Chart 3) allows for the evaluation of sulfur atom influence on the metal-metal electronic coupling.

Chart 3. Indacene and trindene ferrocenyl complexes

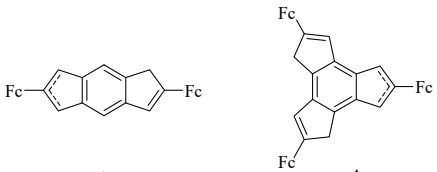

3 **4**

The electrochemical characterization in different media is described. The optical properties of the mixed valence and of the fully oxidized species, selectively generated by chemical oxidation using ferrocenium and acetylferrocenium(BF_4) as the oxidants, were monitored by vis-NIR spectroscopy. The charge transfer processes are rationalized in the framework of the Hush theory. Given their well-recognized and growing interest as electronic materials as scaffolds for organic conductors, the determination of the degree of the electronic coupling through the **BDT** and **BTT** bridging ligand represents a suitable t for probing the conductive capability of these ligands.

RESULTS AND DISCUSSION

Electrochemistry. Oxidative cyclic voltammetry (CV) of **1** and **2** recorded under argon in CH_2Cl_2/0.1 M nBu$_4$NB(C_6F_5)$_4$, (Figures 1a,c). Large waves with oxidation potential maximum at 0.27 (**1**) and 0.24 V (**2**) are present.

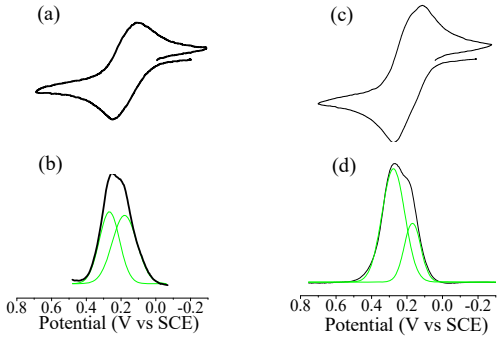

Figure 1. Oxidative CV at 20 °C of **1** (a) and **2** (c) at scan rate 0.5 Vs^{-1}. DPV of **1** (b) and **2** (d). Solvent CH_2Cl_2, supporting electrolyte 0.1 M nBu$_4$NB(C_6F_5)$_4$. DPV conditions: modulation amplitude, 5 mV; modulation time, 0.05 s; interval time (Δt), 0.5 s, step potential (E_{step}), 0.005 V; scan rate, $v = E_{step}/\Delta t$, 0.01 V s^{-1}.

We and Ogawa have previously reported that oxidation of **1**[21d,**Errore. Il segnalibro non è definito.**22] and **2**[22] in the presence of the supporting electrolyte nBu$_4$NBF$_4$ containing a strong coordinating anion with a low delocalized negative charge, such as BF_4^-, showed single oxidation waves despite of the number of electro-active ferrocenyl groups. These results indicated that in that medium the ferrocenyl groups of **1** and **2** are electrochemically undistinguished. Similar results were previously found by us for structurally correlated bis(ferrocenyl) complexes of *s*- and *as*- indacenes[20h] and tris(ferrocenyl) derivative of trindene[20d] in the same conditions.

Otherwise, in the presence of nBu$_4$NB(C_6F_5)$_4$ as supporting electrolyte enclosing the feeble ion-pairing and nucleophilic anion $B(C_6F_5)_4^-$ the waves slightly splits into two oxidation processes.[25i,j,27]

In fact, the deconvolution of the differential pulse voltammetric (DPV) measurement of bis(ferrocenyl) complex **1** evidenced two oxidation peaks of equal areas (Figure 1b, green curves) due to two subsequent oxidation processes, **1**/**1**$^+$ and **1**$^+$/**1**$^{2+}$, at potential 0.18 and 0.27 V. At difference, the 2:1 ratio of the deconvoluted DPV peaks displayed by the triferrocenyl complex **2** (Figure 1d, green curves) evidenced that the second oxidation is a two-electron redox process, with an overall two steps three electron oxidation, **2**/**2**$^+$ and **2**$^+$/**2**$^{3+}$, at 0.17 and 0.28 V. The wave separation $\Delta E = E_p^2 - E_p^1$ and the comproportionation equilibrium constant K_c for **2** (ΔE = 110 mV, K_c = 78) are grater than those of **1** (ΔE = 86 mV, K_c = 30), being $K_c = \exp(F\Delta E/RT)$. The ΔE and K_c values are smaller than those found for the related compound **4** (165 mV, K_c = 687)[20d] and **3** (110 mV, K_c = 78)[20h] respectively.

For organic and organometallic systems containing two or more identical redox groups and undergoing electron-transfer reactions, the typical observation is that the second and subsequent redox events occur with greater difficulty than the first. The separation between the standard potentials, ranging from about 0.1 V to over 1 V, is mainly due to electrostatic factors.[20b,28,29] However, as pointed out by Evans[28] there are cases in which the potential differences is so small such that in cy-

clic voltammetry the two electron-transfer processes produce almost a single voltammetric peak. These are examples of "potential compression". At first glance, this situation seems to controvert the electrostatic argument. However, structural changes associated with the electron transfers occur and are usually responsible for potential compression and even inversion.[30] In addition, Sáveant established that the small ΔE and potential inversion found in the oxidation (or reduction) of a series of carotenoids are ruled by large solvation energies stabilizing the dication (or dianion) forms with respect to mixed-valence species.[30]

In the presence study, the magnitude of ΔE is diagnostic for low thermodynamic stability of $\mathbf{1}^+$ and $\mathbf{2}^+$ and indicates that significant disproportionation occurs upon oxidation, taking into account that only 40-50% of the equilibrium species are monocations, according to the related values of K_c.

In a recent review,[31] Winter presented a cautionary reminder against the often claimed direct correlation between ΔE and the degree of electronic coupling, that frequently fails for systems in which the organic bridge actively participates in the redox processes. In these systems, the redox groups are connected by fully π-conjugated bridges, which contribute to the respective frontier orbitals. In such cases, large electronic couplings are observed despite small potential splittings, sometimes even just above the statistical limit, as found for **1**, or below. Actually, we found that the frontier Kohn–Sham MOs of **1** and **2** have a large ligand contribution. [22]

Trustworthy information on metal-metal electronic coupling in $\mathbf{1}^+$ and $\mathbf{2}^+$ can be attained only if the mixed-valent monocations can be selectively generated in solution by examining the charge transfer bands in near infrared (NIR) spectral region.

Optical Spectroscopy. The charge transfer properties of the mono-, di- and trioxidized species obtained from oxidation of complexes **1**–**2** in CH_2Cl_2 / 0.1 M nBu$_4$NB(C$_6$F$_5$)$_4$ have been probed by analysis the spectra in the NIR region (Figure 2).

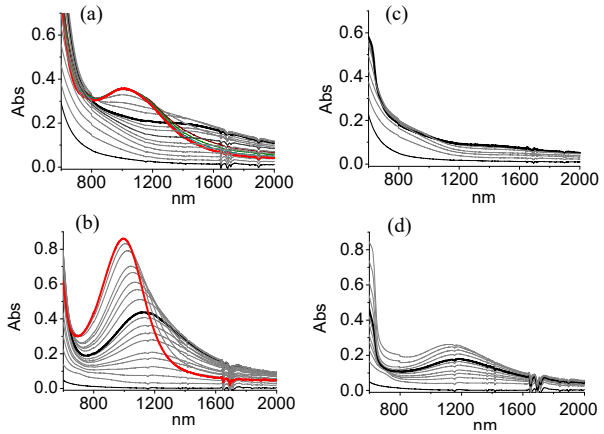

Figure 2. Oxidation of 2.50 mM **1** (a,c) and 2.96 mM of **2** (b,d) solutions in CH_2Cl_2 / 0.1 M nBu$_4$NB(C$_6$F$_5$)$_4$ by incremental addition of acetylferrocenium(BF$_4$) (a,b) or ferrocenium(BF$_4$) (c,d), 1 equiv (black bold line) and 2 (a) or 3 (b) equiv (red bold line).

Oxidation of yellow solutions of **1** and **2** in CH_2Cl_2 / 0.1 M nBu$_4$NPF$_6$ by stepwise addition of acetylferrocenium(BF$_4$) (Supporting Information, Figure S1) produced the fully oxidized cations $\mathbf{1}^{2+}$ and $\mathbf{2}^{3+}$. Otherwise, in the presence of nBu$_4$NB(C$_6$F$_5$)$_4$ as supporting electrolyte, oxidation by incremental addition of acetylferrocenium(BF$_4$) (Figures 2a,b) initially afforded deep green solutions and induced the appearance of energy absorptions at wavelength λ = 1420 and 1180 nm, corresponding to the formation of the monocation $\mathbf{1}^+$ and $\mathbf{2}^+$.

Upon further oxidant addition up to 2 and 3 equivalents, the solutions turned from green to red due to the gradual formation of $\mathbf{1}^{2+}$ and $\mathbf{2}^{3+}$ which absorb at λ = 1010 and 995 nm, respectively.

Interestingly, oxidation by ferrocenium(BF$_4$) of **1** and **2** in the same medium generated more selectively $\mathbf{1}^+$ and $\mathbf{2}^+$ (Figures 2c,d) due to the lower formal oxidation potential of ferrocene with respect to that of acetylferrocene, 0.46 and 0.73 V vs SCE in CH_2Cl_2 / nBu$_4$NPF$_6$, respectively.[32] In addition, we found that in CH_2Cl_2 / 0.1 M nBu$_4$NB(C$_6$F$_5$)$_4$ the oxidation potential of both ferrocene and acetylferrocene decreases of 0.10 V. We attribute the lower energy bands to intervalence charge-transfer (IVCT) transitions.

Gaussian de-convolution of $\mathbf{1}^+$ and $\mathbf{2}^+$ spectra (Figure 3a,c) allowed for the determination of their absorption parameters (Table 1) by using the classical electron transfer Hush model. In particular, the comparison of the experimental and calculated half-bandwidths,[25a] $(\Delta\tilde{\nu}_{1/2})_{Hush}$ (cm^{-1}) = $[16RT\ln 2\,\tilde{\nu}_{max}]^{1/2}$) revealed the narrowness of these bands.

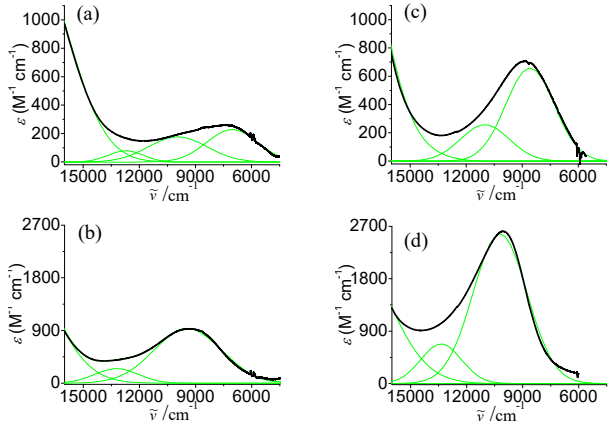

Figure 3. NIR spectra of $\mathbf{1}^+$ (a) $\mathbf{2}^+$ (b), $\mathbf{1}^{2+}$ (c) and $\mathbf{2}^{3+}$ (d) in CH_2Cl_2 / 0.1 M to nBu$_4$NB(C$_6$F$_5$)$_4$ solution at 20 °C (black lines) obtained by oxidation with 1 equiv of acetylferrocenium(BF$_4$). Gaussian deconvolution (green lines) after background subtraction.

The values of $\Gamma = 1-(\Delta\tilde{\nu}_{1/2})_{obsd}/(\Delta\tilde{\nu}_{1/2})_{Hush}$ for $\mathbf{1}^+$ (0.32) and for $\mathbf{2}^+$ (0.42), a criterion proposed by Brunschwig, Creutz and Sutin[25h] to classify the mixed valence species, are larger than those previously found for the structurally related cations of bis(ferrocenyl)-*s*-indacene[20h] $\mathbf{3}^+$ (0.24) and tris(ferrocenyl)-trindene[20d] $\mathbf{4}^+$ (0.27).

These results, besides being consistent with quite strong coupling (Class II mixed-valent cations) greater in $\mathbf{2}^+$ than in $\mathbf{1}^+$, are in favor of a metal-metal electronic coupling stronger in $\mathbf{1}^+$ than in $\mathbf{3}^+$ and in $\mathbf{2}^+$ than in $\mathbf{4}^+$, despite the values of ΔE and K_c found for **1** and **2** being lower than those found for **3** and **4** (Table 1).

The correct evaluation of the electronic coupling $H_{ab} = [0.0205(\varepsilon_{max}\tilde{\nu}_{max}\Delta\tilde{\nu}_{1/2})^{1/2}]/d$, as predicted by the Hush model, is prevented by the relevant narrowness of the low en-

ergy IVCT band for $\mathbf{1}^+$ and $\mathbf{2}^+$ (where *d* is the unknown adiabatic electron transfer distance).[26a]

Finally, the absorption coefficients of the IVCT and LMCT bands found for $\mathbf{2}^+$ and $\mathbf{2}^{3+}$ result almost threefold higher than those of $\mathbf{1}^+$ and $\mathbf{1}^{2+}$ (Table 1).

Table 1. NIR data in CH_2Cl_2.

	$\tilde{\nu}_{max}$ (cm^{-1})	Type	ε_{max} ($M^{-1}cm^{-1}$)	$(\Delta\tilde{\nu}_{1/2})_{obsd}$ (cm^{-1})	$(\Delta\tilde{\nu}_{1/2})_{Hush}$ [a] (cm^{-1})	Γ [b]
$\mathbf{1}^{+}$[c]	7041	IVCT	370[f]	2728	4033	0.32
$\mathbf{1}^{2+}$[c]	9900	LMCT	929	3580		-
$\mathbf{2}^{+}$[c]	8582	IVCT	1095[f]	2602	4474	0.42
$\mathbf{2}^{3+}$[c]	10050	LMCT	2615	2890	-	-
$\mathbf{3}^{+}$[c,d]	5576	IVCT	1286	2690	3590	0.25
$\mathbf{3}^{2+}$[c,d]	9230	LMCT	2930	2600	-	-
$\mathbf{4}^{+}$[c,e]	4875	IVCT	2036	2740	3590	0.24
$\mathbf{4}^{3+}$[c,e]	9670	LMCT	3170	3240	-	-

[a] $(\Delta\tilde{\nu}_{1/2})_{Hush}\ (cm^{-1}) = (16RT\ln 2\tilde{\nu}_{max})^{1/2}$ calculated for the de-convoluted low energy Gaussian component; $T = 20$ °C. [b] $\Gamma = 1-(\Delta\tilde{\nu}_{1/2})_{obsd}/(\Delta\tilde{\nu}_{1/2})_{Hush}$ (ref. 26h). [c] *n*Bu4NB(C_6F_5) as supporting electrolyte. [d] Ref. 20h. [e] Ref. 20d. [f] The concentrations of $\mathbf{2}^+$ and $\mathbf{3}^+$ have been determined taking into account of the dication concentration.

We attribute this effect to the more efficient charge transfer capability of **BTT** with respect to **BDT**. This is not the case for the absorption coefficients of $\mathbf{4}^+$ and $\mathbf{4}^{3+}$ compared to those of $\mathbf{3}^+$ and $\mathbf{3}^{2+}$, indicating less conductive properties of the sulfur-free bridging ligand.

CONCLUSIONS

The optical analysis of the bimetallic and trimetallic cations $\mathbf{1}^+$ and $\mathbf{2}^+$ in the NIR region allowed for the determination of their charge transfer properties and the evaluation of the magnitude of metal-metal electronic coupling. The cations were generated by chemical oxidation using ferrocenium(BF_4) and acetylferrocenium(BF_4) as the oxidants. Ferrocenium(BF_4) produced more selectively $\mathbf{1}^+$ and $\mathbf{2}^+$ due to its formal oxidation potential lower than acetylferrocenium(BF_4), but in poorer amounts.

The CV profiles of **1** and **2** could be switched from a non-resolved two electron oxidation to two processes separated to some extent by changing the anion of the supporting electrolyte from PF_6^- to $B(C_6F_5)_4^-$, the latter having notoriously feeble ion-pairing and nucleophilic capability. Despite the low ΔE splittings, the mixed-valence cation $\mathbf{1}^+$ and $\mathbf{2}^+$ could be selectively generated and analyzed.

Their NIR spectra displayed typical charge transfer bands, which were rationalized in the framework of the Marcus−Hush theory. The IVCT transitions showed astoundingly large Γ values of 0.32 and 0.42, placing these systems well into the regime of rather strongly coupled mixed-valence systems of class II.

Interestingly, the comparison with the results previously found for the structurally related sulfur-free $\mathbf{3}^+$ and $\mathbf{4}^+$ clearly indicates that the sulfur atom strongly increases the metal-metal electronic coupling in $\mathbf{1}^+$ and $\mathbf{2}^+$.

The heteroatom effect is in agreement with the strong conductive properties that are the basis of the preeminent application of **BDT-** and **BTT-**based organic materials.

EXPERIMENTAL SECTION

General Methods. All complex manipulations were performed under an oxygen- and moisture-free atmosphere utilizing standard Schlenk techniques. Solvents were dried by reflux over the appropriate drying agent and distilled under stream of argon. Ferrocene was Sigma Aldrich products. (Acetylferrocenium)(BF_4) was synthesized according to published procedures.[31] CV experiments were performed in an airtight three-electrode cell connected to a vacuum/argon line. The reference electrode was a SCE (Tacussel ECS C10) separated from the solution by a bridge compartment filled with the same solvent/supporting electrolyte solution used in the cell. The counter electrode was a platinum spiral with ca. 1 cm^2 apparent surface area. The working electrodes were disks obtained from cross sections of gold wires of different diameters (0.5 and 0.125 mm) sealed in glass. Between successive CV scans, the working electrodes were polished on alumina according to standard procedures and sonicated before use. An EG&G PAR-175 signal generator was used. The currents and potentials were recorded on a Lecroy 9310L oscilloscope. The potentiostat was home-built with a positive feedback loop for compensation of the ohmic drop.[33] An Autolab PGSTAT 100 potentiostat/galvanostat (EcoChemie, The Netherlands) run by a PC with GPES software was used for the differential pulse voltammetry (DPV) experiments. The measurements were conducted in an airtight three-electrode cell, the same used for the CV experiments. UV−vis and near-IR absorption spectra were recorded with a Varian Cary 5 spectrophotometer.

ASSOCIATED CONTENT

Supporting Information

The Supporting Information is available free of charge on the ACS Publications website.

UV-vis and NIR spectra of $\mathbf{1}^+$ and $\mathbf{2}^+$ in CH_2Cl_2 / *n*Bu_4NPF_6 (PDF)

AUTHOR INFORMATION

Corresponding Author

*Email: saverio.santi@unipd.it

ORCID

Saverio Santi: 0000-0002-6403-4467

Notes

The authors declare no competing financial interest.

ACKNOWLEDGMENT

Financial support by the University of Padova through the grant PRAT 2014 action (2015K7FZLH) is acknowledged.

REFERENCES

1. Wu, W.; Liu, Y.; Zhu, D. Π-Conjugated Molecules with Fused Rings for Organic Field-Effect Transistors: Design, Synthesis and Applications. *Chem. Soc. Rev.* **2010**, *39*, 1489–1502.
2. Mas-Torrent, M.; Rovira, C. Novel Small Molecules for Organic Field-Effect Transistors: Towards Processability and High Performance. *Chem. Soc. Rev.* **2008**, *37*, 827–838.

3. (a) Guo, X.; Wang, S.; Enkelmann, V.; Baumgarten, M.; Müllen, K. Making Benzotrithiophene a Stronger Electron Donor. *Org. Lett.* **2011**, *13*, 6062–6065. (b) Mishra, A.; Ma, C.-Q.; Bäuerle, P. Functional Oligothiophenes: Molecular Design for Multidimensional Nanoarchitectures and Their Applications. *Chem. Rev.* **2009**, *109*, 1141–1276. (c) Katz, H. E.; Lovinger, A. J.; Laquindanum, J. G. α,ω-Dihexylquaterthiophene: A Second Thin Film Single-Crystal Organic Semiconductor. *Chem. Mater.* **1998**, *10*, 457–459.
4. (a) Takimiya, K.; Kato, K.; Aso, Y.; Ogura, F.; Otsubo, T. Synthesis, Structures, and Properties of Two Isomeric Naphthodithiophenes and Their Methyl, Methylthio, and 2-Thienyl Derivatives; Application to Conductive Charge-Transfer Complexes and Low-Bandgap Polymers. *Bull. Chem. Soc. Jpn.* **2002**, *75*, 1795–1805. (b) Takimiya, K.; Otsubo, T.; Ogura, F. Naphtho[1,8-bc : 5,4-b′c′]dithiophene: a new heteroarene isoelectronic with pyrene. *J. Chem. Soc., Chem. Commun.* **1994**, 1859–1860. (c) Takimiya, K.; Yashiki, F.; Aso, Y.; Otsubo, T.; Ogura, F. Facile Preparation and Charge-Transfer Complexes of Naphto[1,8-bc:4,5-b'c']dithiophene and 2,5-Dimethyl(methylthyo) Derivatives. *Chem. Lett.* **1993**, 365–367. (d) Wudl, F.; Haddon, R. C.; Zellers, E. T.; Bramwell, F. B. 3,4:3',4'-Bibenzo[b]thiophene. *J. Org. Chem.* **1979**, *44*, 2491–2493.
5. (a) Chen, M. X.; Perzon, E.; Robisson, N.; Jönsson, S. K. M.; Andersson, M. R.; Fahlman, M.; Berggren, M. Organic Field-Effect Transistors: Towards Molecular Scale. Proceedings of Symposium E. E-MRS Spring Meeting. *Synth. Met.* **2004**, *146*, 233-236. (b) Mazzeo, M.; Vitale, V.; Della Sala, F.; Pisignano, D.; Anni, M.; Barbarella, G.; Favaretto, L.; Zanelli, A.; Cingolani, R.; Gigli, G. New Branched Thiophene-Based Oligomers for Bright Organic Light-Emitting Devices. *Adv. Mater.* **2003**, *15*, 2060–2063.
6. (a) Bronstein, H.; Chen, Z.; Ashraf, R. S.; Zhang, W.; Du, J.; Durrant, J. R.; Tuladhar, P. S.; Song, K.; Watkins, S. E.; Geerts, Y.; Wienk, M. M.; Janssen, R. A. J.; Anthopoulos, T.; Sirringhaus, H.; Heeney, M.; McCulloch, I. Thieno[3,2-b]thiophene−Diketopyrrolopyrrole-Containing Polymers for High-Performance Organic Field-Effect Transistors and Organic Photovoltaic Devices. *J. Am. Chem. Soc.* **2011**, *133*, 3272-3275. (b) Zou, Y.; Najari, A.; Berrouard, P.; Beaupré, S.; Aïch, B. R.; Tao, Y.; Leclerc, M. A Thieno[3,4-c]pyrrole-4,6-dione-Based Copolymer for Efficient Solar Cells. *J. Am. Chem. Soc.* **2010**, *132*, 5330-5331. (c) Zhou, E.; Nakamura, M.; Nishizawa, T.; Zhang, Y.; Wei, Q.; Tajima, K.; Yang, C.; Hashimoto, K. Synthesis and Photovoltaic Properties of a Novel Low Band Gap Polymer Based on N-Substituted Dithieno[3,2-b:2′,3′-d]pyrrole. *Macromolecules* **2008**, 41, 8302-8305. (d) De Bettignies, R.; Nicolas, Y. ; Blanchard, P.; Levillain, E. ; Nunzi, J. M. ; Roncali, J. Planarized Star-Shaped Oligothiophenes as a New Class of Organic Semiconductors for Heterojunction Solar Cells. *Adv. Mater.* **2003**, *15*, 1939–1943.
7. (a) Zhang, G.; Zhu, M.; Guo, J.; Ma, J.; Wang, X.; Lu, H.; Qiu, L. Polypyrrole, α-Fe_2O_3 and Their Hybrid Nanocomposite Sensor: An Impedance Spectroscopy Study. *Organic Electronics* **2014**, *15*, 2608–2615. (b) Guo, X.; Puniredd , S. R.; Baumgarten, M.; Pisula, W.; Müllen, K. Rational Design of Benzotrithiophene-Diketopyrrolopyrrole-Containing Donor-Acceptor Polymers for Improved Charge Carrier Transport. *Adv. Mater.* **2013**, *25*, 5467–5472. (c) Patra, D.; Huang, T.-Y.; Chiang, C.-C.; Maturana, R. O.V.; Pao, C.-W.; Ho, K.-C.; Wei, K.-H; Chu, C.-W. 2-Alkyl-5-thienyl-Substituted Benzo[1,2-b:4,5-b′]dithiophene-Based Donor Molecules for Solution-Processed Organic Solar Cells. *ACS Appl. Mater. Interfaces* **2013**, *5*, 9494–9500. (d) Yamamoto, T.; Takimiya, K. Facile Synthesis of Highly π-Extended Heteroarenes, Dinaphtho[2,3-b:2‘,3‘-f]chalcogenopheno[3,2-b]chalcogenophenes, and Their Application to Field-Effect Transistors. *J. Am. Chem. Soc.* **2007**, *129*, 2224–2225. (e) Zhan, X.; Tan, Z.; Domercq, B.; An, Z.; Zhang, X.; Barlow, S.; Li, Y.; Zhu, D.; Kippelen, B.; Marder, S. R. A High-Mobility Electron-Transport Polymer with Broad Absorption and Its Use in Field-Effect Transistors and All-Polymer Solar Cells. *J. Am. Chem. Soc.* **2007**, *129*, 7246-7247. (f) Zhang, M.; Tsao, H. N.; Pisula, W.; Yang, C.; Mishra, A. K.; Müllen, K. Field-Effect Transistors Based on a Benzothiadiazole−Cyclopentadithiophene Copolymer. *J. Am. Chem. Soc.* **2007**, *129*, 3472-3473. (g) Takimiya, K.; Kunugi, Y.; Toyoshima, Y.; Otsubo, T. 2,6-Diarylnaphtho[1,8-bc:5,4-b‘c‘]dithiophenes as New High-Performance Semiconductors for Organic Field-Effect Transistors. *J. Am. Chem. Soc.* **2005**, *127*, 3605–3612.
8. (a) Rieger, R.; Beckmann, D.; Pisula, W.; Steffen, W.; Marcel Kastler, M.; Műllen, K. Rational Optimization of Benzo[2,1-b;3,4-b′]dithiophene-Containing Polymers for Organic Field-Effect Transistors. *Adv. Mater.* **2010**, *22*, 83–86. (b) S. Ong, B.; Wu, Y. L.; Li, Y. N.; Liu, P.; Pan, H. L. Thiophene Polymer Semiconductors for Organic Thin-Film Transistors. *Chem.–Eur. J.* **2008**, *14*, 4766–4778. (c) McCulloch, I.; Heeney, M.; Bailey, C.; Genevicius, K.; Macdonald, I.; Shkunov, M.; Sparrowe, D.; Tierney, S.; Wagner, R.; Zhang, W. M.; Chabinyc, M. L.; Kline, R. J.; McGehee, M. D.; Toney, M. F. Liquid-Crystalline Semi-Conducting Polymers with High Charge-Carrier Mobility. *Nat. Mater.* **2006**, *5*, 328–333. (d) Li, J.; Qin, F.; Li, C. M.; Bao, Q.; Chan-Park, M. B.; Zhang, W.; Qin, J.; Ong, B.S. High-Performance Thin-Film Transistors from Solution-Processed Dithienothiophene Polymer Semiconductor Nanoparticles. *Chem. Mater.* **2008**, *20*, 2057–2059.
9. (a) Takimiya, K.; Konda, Y.; Ebata, H.; Niihara, N.; Otsubo, T. Facile Synthesis, Structure, and Properties of Benzo[1,2-b:4,5-b‘]dichalcogenophenes. *J. Org. Chem.* **2005**, *70*, 10569–10571. (b) Wang, C. H.; Hu, R. R.; Liang, S.; J. H. Chen, J. H.; Yang, V.; Pei, J. Linear C_2-Symmetric Polycyclic Benzodithiophene: Efficient, Highly Diversified Approaches and the Optical Properties. *Tetrahedron Lett.* **2005**, *46*, 8153–8157. (c) Graupner, W.; Grem, G.; Meghdadi, F.; Paar, C.; Scherf, U.; Mullen, K.; Fischer, W.; Stelzer, F. *Mol. Cryst. Liq. Cryst.* **1994**, *256*, 549–554. (d) Liq, M. C.; Laquindanum, B. J. G.; Katz, H. E.; Lovinger, A. J.; Dodabalapur, A. *Adv. Mater.* Electroluminescence with Conjugated Polymers and Oligomers. (e) Yoshida, S. Fujii, M.; Aso, Y.; Otsubo, T.; Ogura, F. Novel Electron Acceptors Bearing a Heteroquinonoid System. 4. Syntheses, Properties, and Charge-Transfer Complexes of 2,7-Bis(dicyanomethylene)-2,7-dihydrobenzo[2,1-b:3,4-b']dithiophene, 2,7-Bis(dicyanomethylene)-2,7-dihydrobenzo[1,2-b:4,3-b']dithiophene, and 2,6-Bis-(dicyanomethylene)-2,6-dihydrobenzo[1,2-b:4,5-b']dithiophene. *J. Org. Chem.* **1994**, *59*, 3077–3081.
10. Hou, J. H.; Park, M. H.; Zhang, S. Q.; Yao, Y.; Chen, L. M.; Li, J. H.; Yang, Y. Bandgap and Molecular Energy Level Control of Conjugated Polymer Photovoltaic Materials Based on Benzo[1,2-b:4,5-b′]dithiophene. *Macromolecules* **2008**, *41*, 6012−6018.
11. (a) Ye, L.; Zhang, S.; Zhao, W.; Yao, H.; Hou, J. Highly Efficient 2D-Conjugated Benzodithiophene-Based Photovoltaic Polymer with Linear Alkylthio Side Chain. *Chem. Mater.* **2014**, *26*, 3603–3605. (b) Zheng, L.; Chung, Y.-H.; Ma, Y.; Zhang, L.; Xiao, L.; Chen, Z.; Wang, S.; Qu, B.; Gong, Q. A Hydrophobic Hole Ttransporting Oligothiophene for Planar Perovskite Solar Cells with Improved Stability. *Chem. Commun.* **2014**, *50*, 11196–11199. (c) Zhou, J.; Zuo, Y.; Wan, X.; Long, G.; Zhang, Q.; Ni, W.; Liu, Y.; Li, Z.; He, G.; Li, C.; Kan, B.; Li, M.; Chen, Y. Solution-Processed and High-Performance Organic Solar Cells Using Small Molecules with a Benzodithiophene Unit. *J. Am. Chem. Soc.* **2013**, *135*, 8484–8487. (d) Liu, Y.; Wan, X.; Wang, F.; Zhou, J.; Long, G.; Tian, J.; Chen, Y. High-Performance Solar Cells using a Solution-Processed Small Molecule Containing Benzodithiophene Unit. *Adv. Mater.* **2011**, *23*, 5387–5391.
12. (a) Yao, H.; Ye, L.; Zhang, H.; Li, S.; Zhang, S.; Hou, J. Molecular Design of Benzodithiophene-Based Organic Photovoltaic Materials. *Chem. Rev.* **2016**, *116*, 7397−7457. (b) Ye, L.; Zhang, S.; Huo, L.; Zhang, M.; Hou, J. High Performance Photovoltaic Applications Using Solution-Processed Small Molecules. *Acc. Chem. Res.* **2014**, *47*, 1595−1603. (c) Li, M. M.; Ni, W.; Wan, X. J.; Zhang, Q.; Kan, B.; Chen, Y. S. J. Benzo[1,2-b:4,5-b′]dithiophene (BDT)-Based Small Molecules for Solution Pro-

cessed Organic Solar Cells. *Mater. Chem.* A **2015**, *3*, 4765−4776. (d) Huo, L.; Hou, J. Benzo[1,2-b:4,5-b′]dithiophene-Based Conjugated Polymers: Band Gap and Energy Level Control and Their Application in Polymer Solar Cells. *Polym. Chem.* **2011**, *2*, 2453−2461. (e) He, F.; Wang, W.; Chen, W.; Xu, T.; Darling, S. B.; Strzalka, J.; Liu, Y.; Yu, L. Tetrathienoanthracene-Based Copolymers for Efficient Solar Cells. *J. Am. Chem. Soc.* **2011**, *133*, 3284–3287.

13. Rademacher, P.; Heinemann, C.; Jänsch, S.; Kowski, K.; Weiß, M. E. Structural Chemistry of Polycyclic Heteroaromatic Compounds. Part XI. Photoelectron Spectra and Electronic Structures of Tetracyclic Hetarenes of the Triphenylene Type. *Spectrochim. Acta A* **2000**, *56*, 1179–1190.
14. (a) Riaño, A.; Arrechea-Marcos, I.; Mancheño, M. J.; Burrezo, M. P.; De la Peña, A.; Loser, S.; Timalsina, A.; Facchetti, Marks, T. J.; Casado, J.; Navarrete, J. T. L.; Ortiz, R. P.; Segura, J. L. A. Benzotrithiophene versus Benzo/Naphthodithiophene Building Blocks: The Effect of Star-Shaped versus Linear Conjugation on Their Electronic Structures. *Chem.–Eur. J.* **2016**, *22*, 6374–6381. (b) Ringk, A.; Lignie, A.; Hou, Y.; Alshareef, H. N.; Beaujuge, P. M. Short Synthesis of Sulfur Analogues of Polyaromatic Hydrocarbonsthrough Three Palladium-Catalyzed C−H Bond Arylations. *ACS Appl. Mater. Interfaces* **2016**, *8*, 12091 − 12100. (c) Kashiki, T.; Kohara, M.; Osaka, I.; Miyazaki, E.; Takimiya, K. Synthesis and Characterization of Benzo[1,2-b:3,4-b′:5,6-b′′]trithiophene (BTT) Oligomers. *J. Org. Chem.* **2011**, *76*, 4061–4070. (d) Taerum, T.; Lukoyanova, O.; Wylie, R. G.; Perepichka, D. F. Synthesis, Polymerization, and Unusual Properties of New Star-Shaped Thiophene Oligomers- *Org. Lett.* **2009**, *11*, 3230–3233. (e) Nicolas, Y.; Blanchard, P.; Levillain, E.; Allain, M.; Mercier, N.; Roncali, J. Planarized Star-Shaped Oligothiophenes with Enhanced π-Electron Delocalization. *Org. Lett.* **2004**, *6*, 273–276.
15. (a) García-Benito, I.; Zimmermann, I.; Urieta-Mora, J.; Arago, J.; Molina-Ontoria, A.; Ortí, E.; Nazario Martín, N.; Nazeeruddin, M. K. *J.* Isomerism Effect on the Photovoltaic Properties of Benzotrithiophene-Based Hole-Transporting Materials. *Mater. Chem. A* **2017**, *5*, 8317–8324. (b) Molina-Ontoria, A.; Zimmermann García-Benito, I.; Gratia, P.; Roldán-Carmona, C.; Aghazada, S.; Graetzel, M.; Nazeeruddin, M. K.; Martín, N. Benzotrithiophene-Based Hole-Transporting Materials for 18.2 % Perovskite Solar Cells. *Angew. Chem., Int. Ed.* **2016**, *55*, 6270–6274.
16. Cheng, N.; Ma, Y.; Liu, Y.; Zhang, C.; Liu, C. Structures and Photoelectric Properties of Five Benzotrithiophene Isomers-Based Donor–Acceptor Copolymers. *Spectrochim Acta A, Mol. Biomol. Spectrosc*. **2016**, *159*, 262–268.
17. (a) Keshtov, M. L.; Kuklin, S. A.; Kochurov, V. S.; Radychev, N. A.; Zhiyuan Xie, Z.; Khokhlov, A. R. Novel Low-Band-Gap Conjugated Polymers Based on Benzotrithiophene Derivatives for Bulk Heterojunction Solar Cells. *Doklady Chem.* **2015**, *464*, 231–235. (b) Zhao, X.; Yang, D.; Lv, H.; Yind, L.; Yang, X. New Benzotrithiophene Derivative with a Broad Band Gap for High Performance Polymer Solar Cells. *Polym. Chem.* **2013**, *4*, 57–60.
18. Demenev, A.; Eichhorn, S. H.; Taerum, T.; Perepichka, D. F.; Patwardhan, S.; Grozema, F. C.; Siebbeles, L. D. A.; Klenkler, R. Quasi Temperature Independent Electron Mobility in Hexagonal Columnar Mesophases of an H-Bonded Benzotristhiophene Derivative. *Chem. Mater.*, **2010**, *22*, 1420-1428.
19. (a) Weiss, J. Supramolecular Approaches to Nano and Molecular Electronics. *Coord. Chem. Rev.* **2010**, *254*, 2247–2446. (b) Fukino, T.; Fujita, N.; Aida, T. Coupling of a C2-Chiral Ferrocene with Phenylalkynyl Groups: Novel Ferrocenophanes Carrying Multiple Chiral Ferrocenyl Units. *Org. Lett.* **2010**, *12*, 3074–3077. (c) Chebny, V. J.; Dhar, D.; Lindeman, S. V.; Rathore, R. Simultaneous Ejection of Six Electrons at a Constant Potential by Hexakis(4-ferrocenylphenyl)benzene. *Org. Lett.* **2006**, *8*, 5041–5044.
20. (a) Donoli, A.; Bisello, A.; Cardena, R.; Crisma, M.; Orian, L.; Santi, S. Charge Transfer Properties of Benzo[b]thiophene Ferrocenyl Complexes. *Organometallics* **2015**, *34*, 4451−4463. (b) Santi, S.; Bisello, A.; Cardena, R.; Donoli, A. Key Multi(ferrocenyl) Complexes in the Interplay between Electronic Coupling and Electrostatic Interaction. *Dalton Trans.* **2015**, *44*, 5234–5257. (c) Donoli, A.; Bisello, A.; Cardena, R.; Prinzivalli, C.; Crisma, M.; Santi, S. Charge Transfer Properties in Cyclopenta[l]phenanthrene Ferrocenyl Complexes. *Organometallics* **2014**, *33*, 1135–1143. (d) Donoli, A.; Bisello, A.; Cardena, R.; C Prinzivalli, C.; Santi, S. Charge Transfer Properties of Multi(ferrocenyl)trindenes. *Organometallics* **2013**, *32*, 1029−1036. (e) Gidron, O.; Diskin-Posner, Y.; Bendikov, M. High Charge Delocalization and Conjugation in Oligofuran Molecular Wires. *Chem.–Eur. J.* **2013**, *19*, 13140–13150. (f) Donoli, A.; Marcuzzo, V.; Moretto, A.; Toniolo, C.; Cardena, R.; Bisello, A.; Santi, S. New Bis-ferrocenyl End-Capped Peptides: Synthesis and Charge Transfer Properties. *Biopolymers* **2013**, 100, 14-24 (g) Speck, J. M.; Claus, R.; Hildebrandt, A.; Ru, T.; Erasmus, E.; Van As, L.; Swarts, J. C.; Lang, H. Electron Transfer Studies on Ferrocenylthiophenes: Synthesis, Properties, and Electrochemistr. *Organometallics* **2012**, *31*, 6373−6380. (h) Hildebrandt, A.; Lehrich, S. W.; Schaarschmidt, D.; Jaeschke, R.; Schreiter, K.; Spange, S.; Lang, H. Ferrocenyl Maleimides – Synthesis, (Spectro-)Electrochemistry, and Solvatochromism. *Eur. J. Inorg. Chem.* **2012**, *5*, 1114–1121. (i) Kaleta, K.; Hildebrandt, A.; Strehler, F.; Arndt, P.; Jiao, H.; Spannenberg, A.; Lang, H.; Rosenthal, U. Ferrocenyl-Substituted Metallacycles of Titanocenes: Oligocyclopentadienyl Complexes with Promising Properties. *Angew. Chem. Int. Ed.* **2011**, *50*, 11248–11252. (j) Donoli, A.; Bisello, A.; Cardena, R.; Benetollo, F.; Ceccon, A.; Santi, S. Single Two-Electron Transfers and Successive One-Electron Transfers in Biferrocenyl−Indacene Isomers. *Organometallics* **2011**, *30*, 1116–1121. (k) Wagner, M. A New Dimension in Multinuclear Metallocene Complexes. *Angew. Chem. Int. Ed.* **2006**, *45*, 5916–5918.
21. (a) Miesel, D.; Hildebrandt, A.; Lang, H. Molecular Electrochemistry of Multi-Redox Functionalized 5-Membered Heterocycles. *Curr. Opin. Electrochem.* **2018***, 8*, 39 - 44. (b) Y.-P. Ou, F. Hu, S. Tang, J. Yu, J. Li, F. Zhang, D. Kuang, Benzo[1,2-b;4,5-b′]dithiophene-Bridged Bimetal Complexes with Different Redox-Active Terminals: Syntheses, Characterization and Charge Delocalization Studied by Spectro-Electrochemical and DFT Methods. *J. Organomet.Chem.* **2017**, *843*, 66–74. (c) Y.-P. Ou, J. Zhang, F. Zhang, D. Kuang, F. Hartl, L. Rao, S. H. Liu, Notable Differences between Oxidized Diruthenium Complexes Bridged by Four Isomeric Diethynyl Benzodithiophene Ligands. *Dalton Trans.* **2016**, *45*, 6503–6516. (d) H. Muroaka, Y. Watanabe, A. Takahashi, H. Kamoto, S. Ogawa, Synthesis of New Types of Ferrocene Dimers Bridged by a Fused Oligothiophene Spacer and Study of Their Electrochemical Oxidation Process via a Mixed-Valence State. *Heteroatom Chem.* **2014**, *25*, 473–481.
22. Rossi, S.; Bisello, A.; Cardena, R.; Orian, L.; Santi, S. Benzodithiophene and Benzotrithiophene as π Cores for Two- and Three-Blade Propeller-Shaped Ferrocenyl-Based Conjugated Systems. *Eur. J. Org. Chem.* **2017**, 5966–5974.
23. Kobayashi, K.; N. Kobayashi, N. Synthesis and Self-Association, Absorption, and Fluorescence Properties of Differentially Functionalized Hexakis(p-substituted-phenylethynyl)-benzenes. *J. Org. Chem.* **2004**, *69*, 2487–2497.
24. (a) Ferrocenes: Ligands, Materials and Biomolecules; Stepnicka, P., Ed.; Wiley: Chichester, England, 2008. (b) Kowalski, K.; Linseis, M.; Winter, R. F.; Zabel, M.; Zalis, S.; Kelm, H.; Kruger, H.-J.; Sarkar, B.; Kaim, W. Charge Delocalization in a Heterobimetallic Ferrocene-(vinyl)Ru(CO)Cl($PiPr_3$)$_2$ System. *Organometallics* **2009**, *28*, 4196 - 4209. (c) Nakaya, T.; Namiki, K.; Murata, M.; Kanaizuka, K.; Kurashina, M.; Fujita, T.; Nishihara, H. Electronic Communication in the Mixed-valence States of Cyclobutadienecobalt Complexes having Two Ferrocenes and Two Anthraquinones. *J. Inorg. Organomet. Polym. Mater.* **2008**, *18*, 124 - 130. (d) Zhang, R.; Wang, Z.; Wu, Y.; Fu, H.; Yao, J. A Novel Redox-Fluorescence Switch Based on a Triad Containing

Ferrocene and Perylene Diimide Units. *Org. Lett.* **2008**, *10*, 3065-3068. (e) Debroy, P.; Roy, S. Recent Advances in the Synthesis and Properties of Ferrocenes Having an Unsaturated Backbone. *Coord. Chem. Rev.* **2007**, *251*, 203-211. (f) Caballero, A.; Tàrraga, A.; Velasco, M. D.; Espinosa, A.; Molina P. Multifunctional Linear Triferrocene Derivatives Linked by Oxidizable Bridges: Optical, Electronic, and Cation Sensing Properties. *Org. Lett.* **2005**, *7*, 3171–3174.

25. (a) Sundharamurthi, S.; Sudha, K.; Karthikaikumar, S.; Abinaya, Reddy, V. R.; Kalimuthu, P. Switching of Inter-Valence Charge Transfer in Stimuli-Responsive Bis(ferrocenyl)porphyrin. *New J. Chem.* **2018**, 42, 4742-4747. (b) Wilson, L. E.; Hassenrueck, C.; Winter, R. F.; White, A. J. P.; Albrecht, T.; Long, N. J. Functionalised Biferrocene Systems towards Molecular Electronics. *Eur. J. Inorg. Chem.* **2017**, *2017*, 496−504. (c) Wilson, L. E.; Hassenrueck, C.; Winter, R. F.; White, A. J. P.; Albrecht, T.; Long, N. J. Ferrocene- and Biferrocene-Containing Macrocycles towards Single-Molecule Electronics. *Angew. Chem. Int. Ed.* **2017**, *56*, 6838–6842. (d) Fan, Y.; Li, H.-M.; Zou, G.-D.; Zhang, X.; Pan, Y.-L.; Cao, K.-K.; Zhang, M.-L.; Ma, P.-L.; Lu, H.-T. Diferrocenes Bridged by a Geminal Diethynylethene Scaffold with Varying Pendant Substituents: Electronic Interactions in Cross-Conjugated System. *Organometallics* **2017**, *36*, 4278-4286. (e) Hildebrandt, A.; Khalyfeh, K. A.; Nawroth, J. F.; Jordan, R. Electron Transfer Studies on Conjugated Ferrocenyl-Containing Oligomers. *Organometallics*, **2016**, *35*, 3713–3719. (f) Vecchi, A.; Erickson, N. R.; Sabin, J. R.; Floris, B.; Conte, V.; Venanzi, M.; P. Galloni, P.; Nemykin, V. N. Electronic Properties of Mono-Substituted Tetraferrocenyl Porphyrins in Solution and on a Gold Surface: Assessment of the Influencing Factors for Photoelectrochemical Applications. *Chem.–Eur. J.* **2015**, *21*, 269–279. (g) Pfaff, U.; Filipczyk, G.; Hildebrandt, A.; Korb, M.; Lang, H. 1,3,5-Triferrocenyl-2,4,6-tris(ethynylferrocenyl)-benzene – A New Member of the Family of Multiferrocenyl-functionalized Cyclic Systems. *Dalton Trans.* **2014**, *43*, 16310–16321. (h) Hildebrandt, A.; Lang, H. (Multi)ferrocenyl Five-Membered Heterocycles: Excellent Connecting Units for Electron Transfer Studies. *Organometallics* **2013**, *32*, 5640-5653. (i) Speck, J. M.; Schaarschmidt, D.; Lang, H. Atropisomeric 3,3′,4,4′,5,5′-Hexaferrocenyl-2,2′-bithiophene: Synthesis, Solid-State Structure, and Electrochemistry. *Organometallics* **2012**, *31*, 1975–1982. (j) Hildebrandt, A.; Schaarschmidt, D.; Lang, H. Electronically Intercommunicating Iron Centers in Di- and Tetraferrocenyl Pyrroles. *Organometallics* **2011**, *30,* 556–563. (k) Rohde, G.T.; Sabin, J.R.; Barrett, C.D.; Nemykin, V. N. Long-Range Metal–Metal Coupling in Transition-Metal 5,10,15,20-Tetraferrocenylporphyrins. *New J. Chem.* **2011**, *35*, 1440-1448. (l) Oton, F.; Ratera, I.; Espinosa, A.; Tàrraga, A.; Veciana, J.; Molina, P. Conformationally Modulated Intramolecular Electron Transfer Process in a Diaza[2,2]ferrocenophane. *Inorg. Chem.* **2010**, *49*, 3183-3191. (m) Ding, F.; Wang, H.; Wu, Q.; Van Voorhis, T.; Chen, S.; Konopelski, J. P. Computational Study of Bridge-Assisted Intervalence Electron Transfer. *J. Phys. Chem. A* **2010**, *114*, 6039-6046. (n) Santi, S.; Durante, C.; Donoli, A.; Bisello, A.; Orian, L.; Ceccon, A.; Crociani, L.; Benetollo, F. Mixed Valence Properties in Ferrocenyl-Based Bimetallic FeCp−Indenyl−ML_n Complexes: Effect of the ML_n Group. *Organometallics* **2009**, *28*, 3319-3326. (o) Venkatasubbaiah, K.; Doshi, A.; Nowik, I.; Herber, R. H.; Reingold, A. L.; Jäkle, F. Examination of the Mixed-Valence State of the Doubly Boron-Bridged Diferrocene Cation $[(FeCp)_2\{m\text{-}C_{10}H_6(BPh)_2\}]^+$. *Chem.–Eur. J.* **2008**, *14*, 444–458. (p) Figueira-Duarte, T. M.; Lloveras, V.; Vidal-Gancedo, J.; Gegout, A.; Delavaux-Nicot, B.; Welter, R.; Veciana, J.; Rovira, C.; Nierengarten, J.-F. Changes in Electronic Couplings of Mixed-Valence Systems Due to Through-Space Intramolecular Interactions. *Chem. Commun.* **2007**, 4345–4347. (q) Masuda, Y.; Shimizu, C. Solvent Effect on Intramolecular Electron Transfer Rates of Mixed-Valence Biferrocene Monocation Derivatives. *J. Phys. Chem. A* **2006**, *110*, 7019–7027. (r) Barlow, S.; O'Hare, D. Metal−Metal Interactions in Linked Metallocenes. *Chem. Rev.* **1997**, *97*, 637–670.

26. (a) Hush, N. S. Intervalence-Transfer Absorption. Part 2. Theoretical Considerations and Spectroscopic Data. *Prog. Inorg. Chem.* **1967**, *8*, 391–444. (b) Allen, C. C.; Hush N. S. Intervalence-Transfer Absorption. Part 1. Qualitative Evidence for IntervalenceTransfer Absorption in Inorganic Systems in Solution and in the Solid State. *Prog. Inorg. Chem.* **1967**, *8*, 357–389. (c) Robin, M. B.; Day, P. A Survey and Classification. Advances in Inorganic Chemistry and Radiochemistry. A*dv. Inorg. Chem. Radiochem*. **1967**, *10*, 247-422. (d) Creutz, C. Mixed Valence Complexes of d^5-d^6 Metal Centers. *Prog. Inorg. Chem.* **1983**, *30*, 1-73. (e) Rocha, R. C.; Rein, F. N.; Jude, H.; Shreve, A. P.; Concepcion, J. J.; Meyer, T. J. Observation of Three Intervalence-Transfer Bands for a Class II–III Mixed-Valence Complex of Ruthenium. *Angew. Chem., Int. Ed.* **2008**, *47*, 503-506. (f) Crutchley, R. J. Intervalence Charge Transfer and Electron Exchange Studies of Dinuclear Ruthenium Complexes. *Adv. Inorg. Chem.* **1994**, *41*, 273-325. (g) Demadis, K. D.; Haertshorn, C. M.; Meyer T. J. The Localized-to-Delocalized Transition in Mixed-Valence Chemistry. *Chem. Rev.* **2001**, *101*, 2655-2686. (h) Brunschwig, B. S.; Creutz, C.; Sutin, N. Optical Transitions of Symmetrical Mixed-Valence Systems in the Class II-III Transition Regime. *Chem. Soc. Rev.* **2002**, *31*, 168-184. (i) D'Alessandro, D. M.; Keene F. R. Current Trends and Future Challenges in the Experimental, Theoretical and Computational Analysis of Intervalence Charge Transfer (IVCT) Transitions. *Chem. Soc. Rev.* **2006**, *35*, 424-440. (j) Ceccon, A.; Santi, S.; Orian, L.; Bisello, A. Electronic Communication in Heterobinuclear Organometallic Complexes Through Unsaturated Hydrocarbon Bridges. *Coord. Chem. Rev.* **2004**, *248*, 683-724. (k) Aguirre-Etcheverry, P.; O'Hare, D. Electronic Communication through Unsaturated Hydrocarbon Bridges in Homobimetallic Organometallic Complexes. *Chem. Rev.* **2010,** *110,* 4839-4864. (l) Heckmann, A.; Lambert, C. Organic Mixed-Valence Compounds: A Playground for Electrons and Holes. *Angew. Chem., Int. Ed.* **2012**, *51*, 326-392.

27. (a) Geiger, W. E.; Barriére, F. Organometallic Electrochemistry Based on Electrolytes Containing Weakly-Coordinating Fluoroarylborate Anions. *Acc. Chem. Res.* **2010***, 43,* 1030-1039. (b) D'Alessandro, D. M.; Keene, F. R. A Cautionary Warning on the Use of Electrochemical Measurements to Calculate Comproportionation Constants for Mixed-Valence Compounds. *Dalton Trans.* **2004**, 3950-3954. (c) Santi, S.; Orian, L.; Durante, C.; Bisello, A.; Benetollo, F.; Crociani, L.; Ganis, P.; Ceccon, A. Tuning the Electronic Communication in Heterobimetallic Mixed-Valence Ions of (1-Ferrocenyl)- and (2-Ferrocenyl)indenyl Rhodium Isomers. *Chem.–Eur. J.*, **2007**, *13*, 1955-1968. (d) Santi, S.; Orian, L.; Durante, C.; Bencze, E. Z.; Bisello, A.; Donoli, A.; Benetollo, F.; Crociani, L.; Ceccon, A. Metal–Metal Electronic Coupling in syn and anti Stereoisomers of Mixed-Valent $(FeCp)_2$-, $(RhL_2)_2$-, and $(FeCp)(RhL_2)$-as-Indacenediide Ions. *Chem.–Eur. J.*, **2007**, *13*, 7933-7947. (e) Bruna, S.; Gonzalez-Vadillo, A. M.; Nieto, D.; Pastor, C.; Cuadrado, C. Vinyl-Functionalized Silanes and Disiloxanes with Electronically Communicated Ferrocenyl Units. *Organometallics* **2010**, *29*, 2796-2807. (f) Hildebrandt, A.; Rüffer, T.; Erasmus, E.; Swarts, J. C.; Lang, H. A Star-Shaped Supercrowded 2,3,4,5-Tetraferrocenylthiophene: Synthesis, Solid-State Structure, and Electrochemistry. *Organometallics* **2010**, *29*, 4900-4905. (g) Hildebrandt, A.; Schaarschmidt, D. van As, L.; Swarts, J. C. Lang H. Diferrocenes Containing Thiadiazole Connectivities. *Inorg. Chim. Acta* **2011**, *374*, 112-118.

28. Evans, D. H. One-Electron and Two-Electron Transfers in Electrochemistry and Homogeneous Solution Reactions. *Chem. Rev.* **2008**, *108*, 2113–2144.

29. Hildebrandt, A.; Miesel, D.; Lang, H. Electrostatic Interactions within Mixed-Valent Compounds. *Coord. Chem. Rev.* **2018***, 371*, 56-66.

30. Hapiot, P.; Kispert, L. D.; Konovalov, V. V.; Savéant, J.-M. Single Two-Electron Transfers vs Successive One-Electron Transfers in Polyconjugated Systems Illustrated by the Electrochemical Oxidation and Reduction of Carotenoids. *J. Am. Chem. Soc.* **2001**, *123*, 6669-6677.
31. Winter, R. F. Half-Wave Potential Splittings $\Delta E_{1/2}$ as a Measure of Electronic Coupling in Mixed-Valent Systems: Triumphs and Defeats. *Organometallics*, **2014**, *33*, 4517–4536.
32. Connelly, N. G.; Geiger, W. E. Chemical Redox Agents for Organometallic Chemistry. *Chem. Rev.* **1996**, *96*, 877−910.
33. Amatore, C.; Lefrou, C.; Pflüger, F. On-Line Compensation of Ohmic Drop in Submicrosecond Time Resolved Cyclic Voltammetry at Ultramicroelectrodes. *J. Electroanal. Chem.* **1989**, *270*, 43 - 59.

Table of Contents artwork